

AD-A087 425

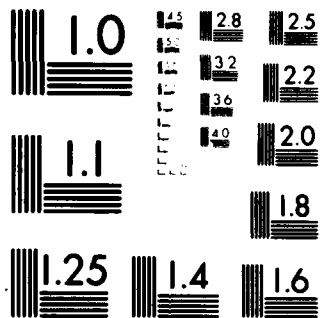
OKLAHOMA UNIV NORMAN SCHOOL OF AEROSPACE MECHANICAL --ETC F/G 11/4
THERMAL BENDING OF THICK RECTANGULAR PLATES OF BIMODULUS COMPOS--ETC(U)
JUN 80 J N REDDY, C W BERT, Y S HSU N00014-78-C-0647
OU-AMNE-80-9 NL

UNCLASSIFIED

10-1
5/2/80



END
DATE
FILMED
9-80
DTIC



MICROCOPY RESOLUTION TEST CHART
NATIONAL BUREAU OF STANDARDS-1963-A

LEVEL II

(12)

Department of the Navy
OFFICE OF NAVAL RESEARCH
Structural Mechanics Program
Arlington, Virginia 22217

Contract N00014-78-C-0647
Project NR 064-609
Technical Report No. 16

Report OU-AMNE-80-9

THERMAL BENDING OF THICK RECTANGULAR PLATES
OF BIMODULUS COMPOSITE MATERIAL

by

J.N. Reddy, C.W. Bert, Y.S. Hsu, and V.S. Reddy

June 1980

DTIC
SELECTED
AUG 4 1980
S A

School of Aerospace, Mechanical and Nuclear Engineering
University of Oklahoma
Norman, Oklahoma 73019

Approved for public release; distribution unlimited

ADA 087425

DDC FILE COPY

80 8 1 01

Accession For

NTIS GRA&I

DDC TAB

Unprocessed

Classification

THERMAL BENDING OF THICK RECTANGULAR PLATES OF BIMODULUS COMPOSITE MATERIALS

J.N. Reddy*, C.W. Bert*, Y.S. Hsu*, and V.S. Reddy**

Publication/

Availability Codes

Available and/or
special

A

↓
Closed-form and finite-element solutions are presented for thermal bending and stretching of laminated composite plates. The material of each layer is assumed to be elastically and thermoelastically orthotropic and bimodular, i.e., having different properties depending upon whether the fiber-direction normal strain is tensile or compressive. The formulations are based on the thermoelastic version of the Whitney-Pagano laminated plate theory, which includes thickness shear deformations. Numerical results are obtained for deflections and neutral-surface positions associated with normal strains in both of the in-plane coordinates. The closed-form and finite-element results are found to be in good agreement.

1 INTRODUCTION

As the use of fiber-reinforced composite materials becomes more widespread, there is ever increasing interest in predicting the thermostructural behavior of plates constructed of such materials. One of the interesting characteristics of certain fiber-reinforced composite materials is that they exhibit quite different elastic properties when loaded along the fiber direction in tension as opposed to compression. This was observed experimentally

* School of Aerospace, Mechanical and Nuclear Engineering, University of Oklahoma, Norman, Oklahoma 73019

** Presently, Structures Engineer, Lear Fan Corp., Reno, Nevada

for cord-rubber composites by Clark (1)[†] and Patel et al. (2). The first attempt to formulate a theory of elastic behavior of such materials was made by Ambartsumyan (3), and a comprehensive theory consistent with experimental results was presented in (4).

Although there have been a number of thermoelastic analyses of bimodulus-material plates (5-9), they have all been limited to isotropic bimodulus materials and temperature changes symmetric about the midplane of the plate. The present work is more general than any existing analyses known to the authors in four different respects:

1. The material of each layer is elastically orthotropic and bimodular.
2. The material of each layer is thermoelastically orthotropic and bimodular, as shown to be possible physically in a recent micromechanics analysis (10).
3. Both single-layer orthotropic and cross-ply laminated plate constructions are considered.
4. Transverse shear deformation is included.
5. Temperature changes through the thickness as well as in the plane are considered.

2 GOVERNING EQUATIONS

The equations developed here constitute the thermoelastic extension of the Whitney-Pagano shear-flexible laminated plate theory (11).

The origin of a Cartesian coordinate system is taken to be in the midplane (xy plane) of the plate with the z axis being normal to this plane and directed downward.

The thermoelastic constitutive relations for each layer (ℓ) are taken to

[†] References are given in Appendix A.

be orthotropic and bimodular as follows:

$$\begin{Bmatrix} \sigma_x \\ \sigma_y \\ \tau_{xy} \end{Bmatrix} = \begin{bmatrix} Q_{11k\ell} & Q_{12k\ell} & 0 \\ Q_{12k\ell} & Q_{22k\ell} & 0 \\ 0 & 0 & Q_{66k\ell} \end{bmatrix} \begin{Bmatrix} \epsilon_x - \alpha_{1k\ell} T \\ \epsilon_y - \alpha_{2k\ell} T \\ \gamma_{xy} \end{Bmatrix} \quad (1)$$

$$\begin{Bmatrix} \tau_{yz} \\ \tau_{xz} \end{Bmatrix} = \begin{bmatrix} C_{440\ell} & 0 \\ 0 & C_{550\ell} \end{bmatrix} \begin{Bmatrix} \gamma_{yz} \\ \gamma_{xz} \end{Bmatrix} \quad (2)$$

Here σ_x and σ_y are in-plane normal stresses, τ_{xy} is in-plane shear stress, τ_{yz} and τ_{xz} are transverse shear stresses, ϵ_x and ϵ_y are in-plane normal strains, γ_{xy} is in-plane engineering shear strain, γ_{yz} and γ_{xz} are transverse engineering shear strains, T is temperature change measured from the strain-free temperature, the C 's are Cauchy elastic shear stiffnesses, the Q 's are plane-stress reduced stiffnesses, and the α 's are thermal-expansion coefficients. The third subscript in $Q_{ijk\ell}$ and $C_{ijk\ell}$ (and second in $\alpha_{jk\ell}$) refers to the bimodular characteristics: $k=1$ denotes properties associated with fiber-direction tension, $k=2$ denotes fiber-direction compression, and $k=0$ signifies that the property does not depend upon fiber-direction strain. Also, subscript ℓ refers to the layer number, i.e., $\ell=1$ and 2 for a two-layer laminate.

The stress resultants and stress couples and thermal stress resultants and couples are defined in the standard manner, i.e.,

$$(N_x, N_y, N_{xy}, Q_y, Q_x) = \int_{-h/2}^{h/2} (\sigma_x, \sigma_y, \tau_{xy}, \tau_{yz}, \tau_{xz}) dz$$

$$(M_x, M_y, M_{xy}) = \int_{-h/2}^{h/2} (\sigma_x, \sigma_y, \tau_{xy}) z dz$$

$$(N_x^T, M_x^T) = \int_{-h/2}^{h/2} (Q_{11k\ell} \alpha_{1k\ell} + Q_{12k\ell} \alpha_{2k\ell})(1, z) T \, dz \quad (3)$$

$$(N_y^T, M_y^T) = \int_{-h/2}^{h/2} (Q_{12k\ell} \alpha_{1k\ell} + Q_{22k\ell} \alpha_{2k\ell})(1, z) T \, dz$$

where h is the total laminate thickness.

The displacements u, v, w in directions x, y, z at an arbitrary location (x, y, z) are given by

$$\begin{aligned} u(x, y, z) &= u^0(x, y) + z\psi_x(x, y) \\ v(x, y, z) &= v^0(x, y) + z\psi_y(x, y) \\ w(x, y, z) &= w^0(x, y) \end{aligned} \quad (4)$$

Here u^0, v^0, w^0 are the displacements at the midplane, and ψ_x and ψ_y are the bending slopes.

Substituting equations (4) into the well-known linear strain-displacement relations of elasticity theory in Cartesian coordinates, and then using equations (1) and (2) in equations (3), one obtains the thermoelastic constitutive relations for the laminate as follows:

$$\begin{Bmatrix} N_x + N_x^T \\ N_y + N_y^T \\ N_{xy} \\ (M_x + M_x^T)/h \\ (M_y + M_y^T)/h \\ M_{xy}/h \end{Bmatrix} = \begin{bmatrix} A_{11} & A_{12} & 0 & B_{11}/h & B_{12}/h & 0 \\ A_{12} & A_{22} & 0 & B_{12}/h & B_{22}/h & 0 \\ 0 & 0 & A_{66} & 0 & 0 & B_{66}/h \\ B_{11}/h & B_{12}/h & 0 & D_{11}/h^2 & D_{12}/h^2 & 0 \\ B_{12}/h & B_{22}/h & 0 & D_{12}/h^2 & D_{22}/h^2 & 0 \\ 0 & 0 & B_{66}/h & 0 & 0 & B_{66}/h^2 \end{bmatrix} \begin{Bmatrix} u_x^0 \\ v_y^0 \\ v_x^0 + u_y^0 \\ h\psi_{x,x} \\ h\psi_{y,y} \\ h\psi_{y,x} + h\psi_{x,y} \end{Bmatrix} \quad (5)$$

$$\begin{Bmatrix} Q_y \\ Q_x \end{Bmatrix} = \begin{bmatrix} S_{44} & 0 \\ 0 & S_{55} \end{bmatrix} \begin{Bmatrix} w_{,y}^0 + \psi_y \\ w_{,x}^0 + \psi_x \end{Bmatrix} \quad (6)$$

Here a comma denotes differentiation, i.e., $(\quad)_{,x} \equiv \partial(\quad)/\partial x$.

As usual, the stretching, bending-stretching coupling, bending and transverse shear stiffnesses for the laminate are defined as

$$(A_{ij}, B_{ij}, D_{ij}, S_{ij}) = \int_{-h/2}^{h/2} (Q_{ij}, Q_{ij}z, Q_{ij}z^2, K_i^2 C_{ij}) dz \quad (7)$$

where K_i^2 is the transverse shear coefficient to provide for the nonuniform transverse-shear strain distribution through the thickness (12).

Neglecting distributed forces, body moments, and inertial effects, one can write the equations of equilibrium as

$$\begin{aligned} N_{x,x} + N_{xy,y} &= 0 ; N_{xy,x} + N_{y,y} = 0 ; Q_{x,x} + Q_{y,y} = 0 \\ M_{x,x} + M_{xy,y} - Q_x &= 0 ; M_{xy,x} + M_{y,y} - Q_y = 0 \end{aligned} \quad (8)$$

Substituting equations (5) and (6) into equations (8), one obtains the following coupled thermoelastic equilibrium equations in terms of the generalized displacements:

$$[L_{kl}] \begin{Bmatrix} u^0 \\ v^0 \\ w^0 \\ h\psi_y \\ h\psi_x \end{Bmatrix} = \begin{Bmatrix} N_{x,x}^T \\ N_{y,y}^T \\ 0 \\ M_{x,x}^T \\ M_{y,y}^T \end{Bmatrix}, \quad (k, l=1, 2, 3, 4, 5) \quad (9)$$

where $[L_{kl}]$ is a symmetrix linear differential operator matrix with the following elements:

$$\begin{aligned}
 L_{11} &\equiv A_{11}d_x^2 + A_{66}d_y^2 & L_{25} &\equiv L_{14} \\
 L_{12} &\equiv (A_{12} + A_{66}) d_x d_y & L_{33} &\equiv -S_{55}d_x^2 - S_{44}d_y^2 \\
 L_{13} &\equiv 0 & L_{34} &\equiv -S_{44}d_y \\
 L_{14} &\equiv (B_{12} + B_{66}) d_x d_y & L_{35} &\equiv -S_{55}d_x \\
 L_{15} &\equiv B_{11}d_x^2 + B_{66}d_y^2 & L_{44} &\equiv D_{66}d_x^2 + D_{22}d_y^2 - S_{44} \\
 L_{22} &\equiv A_{66}d_x^2 + A_{22}d_y^2 & L_{45} &\equiv (D_{12} + D_{66}) d_x d_y \\
 L_{23} &\equiv 0 & L_{55} &\equiv D_{11}d_x^2 + D_{66}d_y^2 - S_{55} \\
 L_{24} &\equiv B_{66}d_x^2 + B_{22}d_y^2 & d_x &\equiv \partial/\partial x .
 \end{aligned} \tag{10}$$

Except for the presence of the generalized thermal-force terms appearing on the right side and the absence of mechanical pressure, equations (9) are identical to those presented recently in (13).

3 CLOSED-FORM SOLUTION

Guided by the closed-form solution presented in (13) for a freely supported, laminated, bimodulus, rectangular plate subjected to a sinusoidally distributed normal pressure, we consider here the same class of plate and geometry but subjected to sinusoidal distributions of midplane temperature and temperature gradient through the thickness. Thus, the temperature distribution is given by

$$T(x,y,z) = T_0(x,y) + (z/h)T_1(x,y) \tag{11}$$

where, here

$$T_0 = \bar{T}_0 \sin \alpha x \sin \beta y, T_1 = \bar{T}_1 \sin \alpha x \sin \beta y \quad (12)$$

$$\alpha = \pi/a, \quad \beta = \pi/b$$

and a and b are the lengths of the plate sides parallel to the x and y axes, respectively.

The boundary conditions are freely supported, i.e., simply supported flexurally and unrestrained in the in-plane directions normal to the edges. Along the edges located at $x=0$ and $x=a$:

$$N_x = v^0 = w = M_x = \psi_y = 0 \quad (13)$$

Along the edges located at $y=0$ and $y=b$:

$$u^0 = N_y = w = M_y = \psi_x = 0 \quad (14)$$

For the temperature distribution and boundary conditions specified above, the governing equations are satisfied exactly in closed form by the following distributions of generalized displacements:

$$\begin{aligned} u^0 &= U \cos \alpha x \sin \beta y \\ v^0 &= V \sin \alpha x \cos \beta y \\ w &= W \sin \alpha x \sin \beta y \\ h\psi_y &= Y \sin \alpha x \cos \beta y \\ h\psi_x &= X \cos \alpha x \cos \beta y \end{aligned} \quad (15)$$

The values of the coefficients U, V, W, Y , and X are obtained by solving the following linear matrix equation obtained by substituting solutions (15) into governing equations (9):

$$[C_{kl}] \begin{Bmatrix} U \\ V \\ W \\ Y \\ X \end{Bmatrix} = \begin{Bmatrix} \bar{N}_{x,x}^T \\ \bar{N}_{y,y}^T \\ 0 \\ \bar{M}_{x,x}^T \\ \bar{M}_{y,y}^T \end{Bmatrix}, \quad (k,l=1,2,3,4,5) \quad (16)$$

where $[C_{kl}]$ is a symmetric matrix containing the following elements:

$$\begin{aligned} C_{11} &\equiv -A_{11}\alpha^2 - A_{66}\beta^2 & C_{25} &\equiv C_{14} \\ C_{12} &\equiv -(A_{12} + A_{66})\alpha\beta & C_{33} &\equiv -S_{55}\alpha^2 - S_{44}\beta^2 \\ C_{13} &\equiv 0 & C_{34} &\equiv -S_{44}\beta \\ C_{14} &\equiv -(B_{12} + B_{66})\alpha\beta & C_{35} &\equiv -S_{55}\alpha^2 \\ C_{15} &\equiv -B_{11}\alpha^2 - B_{66}\beta^2 & C_{44} &\equiv -D_{66}\alpha^2 - D_{22}\beta^2 - S_{44} \\ C_{22} &\equiv -A_{66}\alpha^2 - A_{22}\beta^2 & C_{45} &\equiv -(D_{12} + D_{66})\alpha\beta \\ C_{23} &\equiv 0 & C_{55} &\equiv -D_{11}\alpha^2 - D_{66}\beta^2 - S_{55} \\ C_{24} &\equiv -B_{66}\alpha^2 - B_{22}\beta^2 \end{aligned} \quad (17)$$

and the quantities on the right side are defined by

$$\begin{aligned} \bar{N}_{x,x}^T &= N_{x,x}^T / \cos \alpha x \sin \beta y, \quad \bar{N}_{y,y}^T = N_{y,y}^T / \sin \alpha x \cos \beta y \\ \bar{M}_{x,x}^T &= M_{x,x}^T / \cos \alpha x \sin \beta y, \quad \bar{M}_{y,y}^T = M_{y,y}^T / \sin \alpha x \cos \beta y \end{aligned} \quad (18)$$

Even in the case of a single-layer plate of bimodulus material as considered in (14), the plate stiffnesses A_{ij} , B_{ij} , and D_{ij} depend upon the neutral-surface position (denoted by z_n) associated with the fiber-direction strain. In the case of a cross-ply plate, as considered in (13), these

stiffnesses depend upon both z_{nx} (in the layer oriented in the x direction) and z_{ny} (in the other layer, which is oriented in the y direction). It is noted that the transverse shear stiffnesses are unaffected by z_{nx} and z_{ny} .

To determine the neutral-surface location, we use the kinematics of deformation, i.e.,

$$\epsilon_x = 0 = u_{,x}^0 + z\psi_{x,x} \quad ; \quad \epsilon_y = 0 = v_{,y}^0 + z\psi_{y,y} \quad (19)$$

Then, using equations (15), we obtain

$$\begin{aligned} z_{nx} &= -u_{,x}^0/\psi_{x,x} = -hU/X \\ z_{ny} &= -v_{,y}^0/\psi_{y,y} = -hV/Y \end{aligned} \quad (20)$$

In the present thermoelastic case, not only the A_{ij} , B_{ij} , and D_{ij} stiffnesses depend upon z_{nx} and z_{ny} , but also do the generalized thermal forces N_i^T and M_i^T . The detailed form of these dependences are a function of the nature of the signs of z_{nx} and z_{ny} ; they are developed for various possible cases in Appendix B.

In principle, one could develop a set of explicit relations for determining z_{nx} and z_{ny} . However, the extreme complexity of the algebraic structure of the resulting equation renders this approach impractical. Thus, an iterative procedure analogous to that used in (12,13) for mechanical loading is adopted here. The procedure turns out to be computationally quite efficient.

4 FINITE-ELEMENT FORMULATION

As pointed out in the previous section, an exact closed-form solution to equations (9) can be obtained only under special conditions of geometry, edge conditions, loadings, and lamination. Here we present a simple finite-

element formulation which does not have any limitations (except for those implied in the formulation of the governing equations)(15,16).

Suppose that the region R is subdivided into a finite number N of subregions: finite elements, R_e ($e=1,2,\dots,N$). Over each element the generalized displacements $(u_0, v_0, w, \psi_x, \psi_y)$ are interpolated according to

$$\begin{aligned} u^0 &= \sum_i^r u_i \phi_i^1, & v^0 &= \sum_i^r v_i \phi_i^1, & w^0 &= \sum_i^s w_i \phi_i^2 \\ \psi_x &= \sum_i^p \beta_{x_i} \phi_i^3, & \psi_y &= \sum_i^p \beta_{y_i} \phi_i^3 \end{aligned} \quad (21)$$

where ϕ_i^α ($\alpha=1,2,3$) is the interpolation function corresponding to the i -th node in the element. Note that the in-plane displacements, the transverse displacement, and the slope functions are approximated by different sets of interpolation functions. While this generality is included in the formulation (to indicate the fact that such independent approximations are possible), we dispense with it in the interest of simplicity when the element is actually programmed and take $\phi_i^1 = \phi_i^2 = \phi_i^3$ ($r=s=p$). Here r, s , and p denote the number of degrees of freedom for each variable. That is, the total number of degrees of freedom per element is $2r + s + 2p$.

Substituting equation (21) into the Galerkin integrals associated with the operator equation (9), which must also hold in each element R_e ,

$$\int_{R_e} ([L]\{\delta\} - \{f\})\{\phi\} dx dy = 0 \quad (22)$$

and using integration by parts once (to distribute the differentiation equally between the terms in each expression), we obtain

$$\begin{bmatrix}
 [K^{11}] & [K^{12}] & [K^{13}] & [K^{14}] & [K^{15}] \\
 & [K^{22}] & [K^{23}] & [K^{24}] & [K^{25}] \\
 & & [K^{33}] & [K^{34}] & [K^{35}] \\
 \text{Symmetric} & & & [K^{44}] & [K^{45}] \\
 & & & & [K^{55}]
 \end{bmatrix}
 \begin{Bmatrix}
 \{u^0\} \\
 \{v^0\} \\
 \{w^0\} \\
 \{\psi_x\} \\
 \{\psi_y\}
 \end{Bmatrix}_e
 =
 \begin{Bmatrix}
 \{F^1\} \\
 \{F^2\} \\
 \{F^3\} \\
 \{F^4\} \\
 \{F^5\}
 \end{Bmatrix}_e
 \quad (23)$$

where the $\{u^0\}$, $\{v^0\}$, etc. denote the columns of the nodal values of u^0 , v^0 , respectively, and the elements $K_{ij}^{\alpha\beta}$ ($\alpha, \beta=1,2,\dots,5$) of the symmetric stiffness matrix and F_i^α of the force vector are given by

$$\begin{aligned}
 K_{ij}^{11} &= A_{11}G_{ij}^x + A_{66}G_{ij}^y & K_{ij}^{25} &= B_{66}H_{ij}^x + B_{22}H_{ij}^y \\
 K_{ij}^{12} &= A_{12}G_{ij}^{xy} + A_{66}G_{ji}^{xy} & K_{ij}^{33} &= S_{55}S_{ij}^x + S_{44}S_{ij}^y \\
 K_{ij}^{13} &= 0 & K_{ij}^{34} &= S_{55}R_{ij}^{x0} \\
 K_{ij}^{14} &= B_{11}H_{ij}^x + B_{66}H_{ij}^y & K_{ij}^{35} &= S_{44}R_{ij}^{y0} \\
 K_{ij}^{15} &= B_{12}H_{ij}^{xy} + B_{66}H_{ji}^{xy} & K_{ij}^{44} &= D_{11}T_{ij}^x + D_{66}T_{ij}^y + S_{55}T_{ij}^0 \\
 K_{ij}^{22} &= A_{22}G_{ij}^y + A_{66}G_{ij}^x & K_{ij}^{45} &= D_{12}T_{ij}^{xy} + D_{66}T_{ji}^{xy} \\
 K_{ij}^{23} &= 0 & K_{ij}^{55} &= D_{66}T_{ij}^x + D_{22}T_{ij}^y + S_{44}T_{ij}^0 \\
 K_{ij}^{24} &= B_{66}H_{ij}^{xy} + B_{12}H_{ji}^{xy}
 \end{aligned}
 \quad (24)$$

$$\begin{aligned}
 F_i^1 &= \int_{R_e} N_{x\phi_i}^T dx dy & F_i^4 &= \int_{R_e} M_{x\phi_i}^T dx dy \\
 F_i^2 &= \int_{R_e} N_{y\phi_i}^T dx dy & F_i^5 &= \int_{R_e} M_{y\phi_i}^T dx dy \\
 F_i^3 &= 0
 \end{aligned}
 \quad (25)$$

where

$$\begin{aligned}
 G_{ij}^{\xi n} &= \int_{R_e} \phi_{i,\xi}^1 \phi_{j,n}^1 dx dy & (i,j=1,2,\dots,r) \\
 H_{ij}^{\xi n} &= \int_{R_e} \phi_{i,\xi}^1 \phi_{j,n}^3 dx dy & (i=1,2,\dots,r ; j=1,2,\dots,t) \\
 M_{ij}^{\xi n} &= \int_{R_e} \phi_{i,\xi}^1 \phi_{j,n}^2 dx dy & (i=1,2,\dots,r ; j=1,2,\dots,s) \\
 S_{ij}^{\xi n} &= \int_{R_e} \phi_{i,\xi}^2 \phi_{j,n}^2 dx dy & (i,j=1,2,\dots,s) \\
 R_{ij}^{\xi n} &= \int_{R_e} \phi_{i,\xi}^2 \phi_{j,n}^3 dx dy & (i=1,2,\dots,s ; j=1,2,\dots,t) \\
 T_{ij}^{\xi n} &= \int_{R_e} \phi_{i,\xi}^3 \phi_{j,n}^3 dx dy & (i,j=1,2,\dots,s)
 \end{aligned} \tag{26}$$

($\xi, n=0, x, y$)

and $G_{ij}^{xx} = G_{ij}^x$, etc. In the special case in which $\phi_i^1 = \phi_i^2 = \phi_i^3$, all of the matrices in equation (26) coincide.

In the present study, elements of the serendipity family are employed with the same interpolation for all of the variables. The resulting stiffness matrices are 20 by 20 for this four-node element and 40 by 40 for the eight-node element. Reduced integration (17,18) must be used to evaluate the matrix coefficients in equation (24). That is, if the four-node rectangular element is used, the 1x1 Gauss rule must be used in place of the standard 2x2 Gauss rule to numerically evaluate the coefficients K_{ij} .

Substituting solution (23) into equations (20), we get

$$z_{nx}^e = -(u_{,x}^0)^e / \psi_{x,x}^e ; \quad z_{ny}^e = -(v_{,y}^0)^e / \psi_{y,y}^e$$

5 NUMERICAL RESULTS

As a check on the validity of the equations and their computational implementation, it is desirable to compare the present predictions with those given in the literature for special cases. Apparently there is a dearth of solutions of plates bent by a sinusoidally distributed thermal gradient. However, it was possible to compare with isotropic, thin plate results given by Boley and Weiner (19) as listed in Table 1. As can be seen, the agreement is quite good.

As examples of orthotropic bimodulus materials, the same materials as considered in (13,14) are used, namely, aramid-rubber and polyester-rubber. The elastic properties, obtained from experimental results of (2) using the data-reduction procedure presented in (4), are listed in Table 2. Unfortunately there are no measured values available for the thermal-expansion coefficients of these materials. However, the micromechanics analysis of bimodular action presented in (10) suggests that the thermal-expansion coefficients of these materials should also depend upon the sign of the fiber-direction strain. Thus, for the numerical calculations presented here, it is assumed that the following relationships hold:

$$\alpha_1^t/\alpha_1^c = 0.5 ; \alpha_2^t/\alpha_2^c = 1.0 ; \alpha_1^t/\alpha_2^t = 0.1$$

Numerical results are presented for relatively thick plates ($b/h=10$) with a temperature distribution having a temperature gradient through the thickness but no mean temperature change, i.e., $\bar{T}_0=0$. Table 3 gives results for single-layer orthotropic plates of various aspect ratios.

As can be seen, there is good agreement between both dimensionless deflections and neutral-surface locations as predicted by the finite-element

and closed-form solutions. In fact, the largest difference appearing in the table are 0.15% for \bar{W} , 0.18 for Z_x , and 1.3% for Z_y .

Table 4 shows the finite-element and closed-form solutions for dimensionless deflections and neutral-surface locations of two-layer cross-ply ($0^\circ/90^\circ$) simply-supported rectangular plates subjected to sinusoidal thermal loading. The finite-element results are in close agreement with the closed-form results.

It should be mentioned that composite materials typically have much lower ratios of thickness shear moduli to in-plane Young's moduli than homogeneous, isotropic materials ($G/E = 1/3$ to $1/2$). In contrast, aramid-rubber has $G_{xz}/E_x = 0.001$ when the fiber-direction strain is tensile, but 0.416 for compressive fiber-direction strain.

Figure 1 presents the influence of the aspect ratio and side-to-thickness ratio for single-layer and two-layer cross-ply plates under sinusoidal thermal loading (material: polyester-rubber). The effect of thickness on the deflection is more pronounced than the effect of the aspect ratio.

Figures 2 and 3 show the effect of the aspect ratio (a/b) and side-to-thickness ratio (b/t), respectively, on the location of neutral surfaces for a single-layer, orthotropic, bimodulus, simply supported rectangular plates under sinusoidal thermal loading (material: aramid-rubber, $\bar{T}_0=0.0$, $\bar{T}_1=1.0$).

Similar results are presented in Figures 4 and 5 for a two-layer cross-ply ($0^\circ/90^\circ$), rectangular plate of polyester-rubber under sinusoidal thermal loading. Note from Figure 5 that the neutral-surface locations are virtually unchanged for side-to-thickness ratio greater than 25.

6 CONCLUSIONS

On the basis of the excellent comparisons with existing results for homogeneous-material plates and the comparisons with a closed-form solution for laminated bimodulus composite-material plates, the mixed finite element for thick plates as presented here is considered to be validated.

7 ACKNOWLEDGMENTS

The authors are grateful to the Office of Naval Research, Structural Mechanics Program for financial support through Contract N00014-78-C-0647 and to the University's Merrick Computing Center for providing computing time.

APPENDIX A

REFERENCES

- (1) CLARK, S.K., 'The plane elastic characteristics of cord-rubber laminates', *Textile Research J.* 1963 33, 295-313.
- (2) PATEL, H.P., TURNER, J.L., and WALTER, J.D., 'Radial tire cord-rubber composites', *Rubber Chem. and Tech.* 1976 49, 1095-1110.
- (3) AMBARTSUMYAN, S.A., 'The basic equations and relations of the different-modulus theory of elasticity of an anisotropic body', *Mechanics of Solids* 1969 4 (No. 3), 48-56.
- (4) BERT, C.W., 'Models for fibrous composites with different properties in tension and compression', *J. Eng. Matls. and Tech., Trans. ASME* 1977 99H, 344-349.
- (5) AMBARTSUMYAN, S.A., 'The equations of temperature stresses of different-modulus materials', *Mechanics of Solids* 1968 3 (No. 5), 58-69.
- (6) AMBARTSUMYAN, S.A., 'Equations of theory of thermal stresses in double-modulus materials', in BOLEY, B.A. (ed.), *Thermoelasticity* (Proc., IUTAM Sympos., E. Kilbride, Scotland, June 25-28, 1968) 1970, 17-32, Springer-Verlag, Wien.
- (7) KAMIYA, N., 'Thermal stress in a bimodulus thin plate', *Bulletin de l'academie Polonaise des Sciences, Serie des sciences techniques* 1976 24, 365-372.
- (8) KAMIYA, N., 'Energy formulae of bimodulus material in thermal field', *Fibre Sci. and Tech.* 1978 11, 229-235.

- (9) KAMIYA, N., 'Bimodulus thermoelasticity considering temperature-dependent material properties', BERT, C.W. (ed.), *Mechanics of Bimodulus Materials* Dec. 2-7, 1979, 29-37, ASME Winter Annual Meeting, New York.
- (10) BERT, C.W., 'Micromechanics of the different elastic behavior of filamentary composite in tension and compression', in BERT, C.W. (ed.), *Mechanics of Bimodulus Materials* Dec. 2-7, 1979, 17-28, ASME Winter Annual Meeting, New York.
- (11) WHITNEY, J.M. and PAGANO, N.J., 'Shear deformation in heterogeneous anisotropic plates', *J. Appl. Mech.* 1970 37, 1031-1036.
- (12) WHITNEY, J.M., 'Shear correction factors for orthotropic laminates under static loads', *J. Appl. Mech.* 1973 40, 302-304.
- (13) BERT, C.W., REDDY, J.N., REDDY, V.S., and CHAO, W.C., 'Analysis of thick rectangular plates laminated of bimodulus composite materials', *AIAA/ASME/ASCE/AHS 21st Structures, Structural Dynamics and Materials Conference*, Seattle, May 12-14, 1980.
- (14) BERT, C.W. and KINCANNON, S.K., 'Bending-extensional coupling in elliptic plates of orthotropic bimodulus material', *Developments in Mechanics*, 10 (Proc., 16th Midwestern Mechanics Conference, Sept. 19-21, 1979), 7-11, Kansas State Univ., Manhattan, Kansas.
- (15) REDDY, J.N., 'A penalty plate-bending element for the analysis of laminated anisotropic composite plates', *Int. J. Numer. Meth. Engng.* 1980, in press.
- (16) REDDY, J.N. and HSU, Y.S., 'Effects of shear deformation and anisotropy on the thermal response of layered composite plates', *J. Thermal Stresses*, to appear.
- (17) ZIENKIEWICZ, O.C., TAYLOR, R.L., and TOO, J.M., 'Reduced integration technique in general analysis of plates and shells', *Int. J. Numer. Meth. Engng.* 1971 3, 575-586.
- (18) REDDY, J.N., 'A comparison of closed-form and finite-element solutions of thick, laminated, anisotropic rectangular plates', *Report OU-AMNE-79-19*, University of Oklahoma, Norman, OK, Dec. 1979.
- (19) BOLEY, B.A. and WEINER, J.H., *Theory of Thermal Stresses*, Wiley, New York, 1960, 389-391.

APPENDIX B

DERIVATION OF EXPRESSIONS FOR THERMAL FORCES AND MOMENTS

Case I

For Case I, $z_{nx} > 0$ and $z_{ny} < 0$ with z_{nx} governing layer 1 (0°) and z_{ny}

layer 2 (90°).

$$N_x^T = \int_{-h/2}^{z_{ny}} (Q_{1122} \alpha_{122} + Q_{1222} \alpha_{222})^T dz + \int_{z_{ny}}^0 (Q_{1112} \alpha_{112} + Q_{1212} \alpha_{212})^T dz \quad (B-1)$$

$$+ \int_0^{z_{nx}} (Q_{1121} \alpha_{121} + Q_{1221} \alpha_{221})^T dz + \int_{z_{nx}}^{h/2} (Q_{1111} \alpha_{111} + Q_{1211} \alpha_{211})^T dz$$

Let

$$(Q_{1122} \alpha_{122} + Q_{1222} \alpha_{222}) = \beta_{122} \quad , \quad (Q_{1112} \alpha_{112} + Q_{1212} \alpha_{212}) = \beta_{112} \quad (B-2)$$

$$(Q_{1121} \alpha_{121} + Q_{1221} \alpha_{221}) = \beta_{121} \quad , \quad (Q_{1111} \alpha_{111} + Q_{1211} \alpha_{211}) = \beta_{111} \quad , \text{ etc.}$$

Then,

$$N_x^T = [\beta_{122} T_o(z_{ny} + h/2) + \beta_{112} T_o(0 - z_{ny}) + \beta_{121} T_o(z_{nx} - 0)$$

$$+ \beta_{111} T_o(h/2 - z_{nx}) + \beta_{122}(T_1/2h)(z_{ny}^2 - h^2/4)$$

$$+ \beta_{112}(T_1/2h)(0 - z_{ny}^2) + \beta_{121}(T_1/2h)(z_{nx}^2 - 0)$$

$$+ \beta_{111}(T_1/2h)(h^2/4 - z_{nx}^2)] \sin \alpha x \sin \beta y$$

or

$$N_x^T = [(\beta_{122} + \beta_{111})(T_o h/2) + (\beta_{121} - \beta_{111}) T_o z_{nx} + (\beta_{122} - \beta_{112}) T_o z_{ny}$$

$$+ (\beta_{111} - \beta_{122})(T_1 h/8) + (\beta_{121} - \beta_{111})(T_1 z_{nx}^2/2h)$$

$$+ (\beta_{122} - \beta_{112})(T_1 z_{ny}^2/2h)] \sin \alpha x \sin \beta y \quad (B-3)$$

Similarly,

$$\begin{aligned}
N_y^T = & [(\beta_{222} + \beta_{211})(T_0 h/2) + (\beta_{221} - \beta_{211}) T_0 z_{nx} + (\beta_{222} - \beta_{212}) T_0 z_{ny} \\
& + (\beta_{211} - \beta_{222})(T_1 h/8) + (\beta_{221} - \beta_{211})(T_1 z_{nx}^2/2h) + (\beta_{222} - \beta_{212}) \\
& (T_1 z_{ny}^2/2h)] \sin \alpha x \sin \beta y
\end{aligned} \tag{B-4}$$

Now,

$$\begin{aligned}
M_x^T = & \int_{-h/2}^{h/2} \beta_{122} T z \, dz + \int_{z_{ny}}^0 \beta_{112} T z \, dz + \int_0^{z_{nx}} \beta_{121} T z \, dz + \int_{z_{nx}}^{h/2} \beta_{111} T z \, dz \\
& [(\beta_{111} - \beta_{122})(T_0 h^2/8) + (\beta_{121} - \beta_{111})(T_0 z_{nx}^2/2) + (\beta_{122} - \beta_{112})(T_0 z_{ny}^2/2) \\
& + (\beta_{122} + \beta_{111})(T_1 h^2/24) + (\beta_{121} - \beta_{111})(T_1 z_{nx}^3/3h) \\
& + (\beta_{122} - \beta_{112})(T_1 z_{ny}^3/3h)] \sin \alpha x \sin \beta y
\end{aligned} \tag{B-5}$$

Similarly,

$$\begin{aligned}
M_y^T = & [(\beta_{211} - \beta_{222})(T_0 h^2/8) + (\beta_{221} - \beta_{211})(T_0 z_{nx}^2/2) + (\beta_{222} - \beta_{212})(T_0 z_{ny}^2/2) \\
& + (\beta_{222} + \beta_{211})(T_1 h^2/24) + (\beta_{221} - \beta_{212})(T_1 z_{nx}^3/3h) \\
& + (\beta_{222} - \beta_{212})(T_1 z_{ny}^3/3h)] \sin \alpha x \cos \beta y
\end{aligned} \tag{B-6}$$

Using the above equations in conjunction with equations (12) and (18), we obtain the following:

$$\begin{aligned}
N_{x,x}^T = & \alpha [(\beta_{122} + \beta_{111})(T_0 h/2) + (\beta_{121} - \beta_{111}) T_0 z_{nx} + (\beta_{122} - \beta_{112}) T_0 z_{ny} \\
& + (\beta_{111} - \beta_{122})(T_1 h/8) + (\beta_{121} - \beta_{111})(T_1 z_{nx}^2/2h) \\
& + (\beta_{122} - \beta_{112})(T_1 z_{ny}^2/2h)]
\end{aligned} \tag{B-7}$$

$$\begin{aligned}\bar{N}_{t,y}^T = & \beta[(\beta_{222} + \beta_{211})(\tau_0 h/2) + (\beta_{221} - \beta_{211})\tau_0 z_{nx} + (\beta_{222} - \beta_{212})\tau_0 z_{ny} \\ & + (\beta_{211} - \beta_{222})(\tau_1 h/8) + (\beta_{221} - \beta_{211})(\tau_1 z_{nx}^2/2h) \\ & + (\beta_{222} - \beta_{212})(\tau_1 z_{ny}^2/2h)]\end{aligned}\quad (B-8)$$

$$\begin{aligned}\bar{M}_{x,x}^T = & \alpha[(\beta_{111} - \beta_{122})(\tau_0 h^2/8) + (\beta_{121} - \beta_{111})(\tau_0 z_{nx}^2/2) + (\beta_{122} - \beta_{112}) \\ & (\tau_0 z_{ny}^2/2) + (\beta_{122} + \beta_{111})(\tau_1 h^2/24) + (\beta_{121} - \beta_{111})(\tau_1 z_{nx}^3/3h) \\ & + (\beta_{122} - \beta_{112})(\tau_1 z_{ny}^3/3h)]\end{aligned}\quad (B-9)$$

$$\begin{aligned}\bar{M}_{y,y}^T = & \beta[(\beta_{211} - \beta_{222})(\tau_0 h^2/8) + (\beta_{221} - \beta_{211})(\tau_0 z_{nx}^2/2) + (\beta_{222} - \beta_{212})(\tau_0 z_{ny}^2/2) \\ & + (\beta_{222} + \beta_{211})(\tau_1 h^2/24) + (\beta_{221} - \beta_{211})(\tau_1 z_{nx}^3/3h) + (\beta_{222} - \beta_{212})(\tau_1 z_{ny}^3/3h)]\end{aligned}\quad (B-10)$$

In a similar way, one can obtain the expressions for the above-mentioned quantities for the remaining seven cases as follows:

Case II ($z_{nx} > 0, z_{ny} > 0$)

$$\begin{aligned}\bar{N}_{x,x}^T = & \alpha[(\beta_{122} + \beta_{111})(\tau_0 h/2) + (\beta_{121} - \beta_{111})(\tau_0 z_{nx}) \\ & + (\beta_{111} - \beta_{122})(\tau_1 h/8) + (\beta_{121} - \beta_{111})(\tau_1 z_{nx}^2/2h)] \\ \bar{N}_{y,y}^T = & \beta[(\beta_{222} + \beta_{211})(\tau_0 h/2) + (\beta_{221} - \beta_{211})(\tau_0 z_{nx}) \\ & + (\beta_{211} - \beta_{222})(\tau_1 h/8) + (\beta_{221} - \beta_{211})(\tau_1 z_{nx}^2/2h)] \\ \bar{M}_{x,x}^T = & \alpha[(\beta_{111} - \beta_{122})(\tau_0 h^2/8) + (\beta_{121} - \beta_{111})(\tau_0 z_{nx}^2/2) \\ & + (\beta_{122} + \beta_{111})(\tau_1 h^2/24) + (\beta_{121} - \beta_{111})(\tau_1 z_{nx}^3/3h)] \\ \bar{M}_{y,y}^T = & \beta[(\beta_{211} - \beta_{222})(\tau_0 h^2/8) + (\beta_{221} - \beta_{211})(\tau_0 z_{nx}^2/2) \\ & + (\beta_{222} - \beta_{211})(\tau_1 h^2/24) + (\beta_{221} - \beta_{211})(\tau_1 z_{nx}^3/3h)]\end{aligned}\quad (B-11)$$

Case III ($z_{nx} < 0, z_{ny} > 0$)

$$\begin{aligned}\bar{N}_{x,x}^T = & \alpha[(\beta_{122} + \beta_{111})(\bar{T}_0 h/2) + (\beta_{121} - \beta_{111})(\bar{T}_0 z_{ny}) \\ & + (\beta_{122} - \beta_{112})(\bar{T}_0 z_{nx}) + (\beta_{111} - \beta_{122})(\bar{T}_1 h/8) \\ & + (\beta_{121} - \beta_{111})(\bar{T}_1 z_{ny}^2/2h) + (\beta_{122} - \beta_{112})(\bar{T}_1 z_{nx}^2/2h)]\end{aligned}$$

$$\begin{aligned}\bar{N}_{y,y}^T = & \beta[(\beta_{222} + \beta_{211})(\bar{T}_0 h/2) + (\beta_{221} - \beta_{211})(\bar{T}_0 z_{ny}) \\ & + (\beta_{222} - \beta_{212})(\bar{T}_0 z_{nx}) + (\beta_{211} - \beta_{222})(\bar{T}_1 h/8) \\ & + (\beta_{221} - \beta_{211})(\bar{T}_1 z_{ny}^2/2h) + (\beta_{222} - \beta_{212})(\bar{T}_1 z_{nx}^2/2h)]\end{aligned}$$

(B-12)

$$\begin{aligned}\bar{M}_{x,x}^T = & \alpha[(\beta_{111} - \beta_{122})(\bar{T}_0 h^2/8) + (\beta_{121} - \beta_{111})(\bar{T}_0 z_{ny}^2/2) \\ & + (\beta_{122} - \beta_{112})(\bar{T}_0 z_{nx}^2/2) + (\beta_{122} + \beta_{111})(\bar{T}_1 h^2/24) \\ & + (\beta_{121} - \beta_{111})(\bar{T}_1 z_{ny}^3/3h) + (\beta_{122} - \beta_{112})(\bar{T}_1 z_{nx}^3/3h)]\end{aligned}$$

$$\begin{aligned}\bar{M}_{y,y}^T = & [(\beta_{211} - \beta_{222})(\bar{T}_0 h^2/8) + (\beta_{221} - \beta_{211})(\bar{T}_0 z_{ny}^2/2) \\ & + (\beta_{222} - \beta_{212})(\bar{T}_0 z_{nx}^2/2) + (\beta_{222} + \beta_{211})(\bar{T}_1 h^2/24) \\ & + (\beta_{221} - \beta_{211})(\bar{T}_1 z_{ny}^3/3h) + (\beta_{222} - \beta_{212})(\bar{T}_1 z_{nx}^3/3h)]\end{aligned}$$

Case IV ($z_{nx} < 0, z_{ny} < 0$)

$$\begin{aligned}\bar{N}_{x,x}^T = & \alpha[(\beta_{122} + \beta_{111})(\bar{T}_0 h/2) + (\beta_{122} - \beta_{121})(\bar{T}_0 z_{ny}) \\ & + (\beta_{111} - \beta_{122})(\bar{T}_1 h/8) + (\beta_{122} - \beta_{121})(\bar{T}_1 z_{ny}^2/2h)]\end{aligned}$$

$$\begin{aligned}\bar{N}_{y,y}^T = & \beta[(\beta_{222} + \beta_{211})(\bar{T}_0 h/2) + (\beta_{222} - \beta_{221})(\bar{T}_0 z_{ny}) \\ & + (\beta_{211} - \beta_{222})(\bar{T}_1 h/8) + (\beta_{222} - \beta_{221})(\bar{T}_1 z_{ny}^2/2h)]\end{aligned}$$

$$\begin{aligned}
\bar{M}_{x,x}^T &= \alpha[(\beta_{111} - \beta_{122})(\bar{T}_0 h^2/8) + (\beta_{122} - \beta_{121})(\bar{T}_0 z_{ny}^2/2) \\
&\quad + (\beta_{122} + \beta_{111})(\bar{T}_1 h^2/24) + (\beta_{122} - \beta_{121})(\bar{T}_1 z_{ny}^3/3h)] \\
\bar{M}_{y,y}^T &= \beta[(\beta_{211} - \beta_{222})(\bar{T}_0 h^2/8) + (\beta_{222} - \beta_{221})(\bar{T}_0 z_{ny}^2/2) \\
&\quad + (\beta_{222} + \beta_{211})(\bar{T}_1 h^2/24) + (\beta_{222} - \beta_{221})(\bar{T}_1 z_{ny}^3/3h)]
\end{aligned} \tag{B-13}$$

For neutral surface going out of plane,

Case V ($z_{nx} > 0.5$, $z_{ny} < -0.5$)

$$\begin{aligned}
\bar{N}_{x,x}^T &= \alpha[(\beta_{121} + \beta_{112})(\bar{T}_0/2) + (\beta_{121} - \beta_{112})(\bar{T}_1/8)] \\
\bar{N}_{y,y}^T &= \beta[(\beta_{221} + \beta_{212})(\bar{T}_0/2) + (\beta_{221} - \beta_{212})(\bar{T}_1/8)] \\
\bar{M}_{x,x}^T &= \alpha[(\beta_{121} - \beta_{112})(\bar{T}_0/8) + (\beta_{121} + \beta_{112})(\bar{T}_1/24)] \\
\bar{M}_{y,y}^T &= \beta[(\beta_{221} - \beta_{212})(\bar{T}_0/8) + (\beta_{221} + \beta_{212})(\bar{T}_1/24)]
\end{aligned} \tag{B-14}$$

Case VI ($z_{nx} < -0.5$, $z_{ny} > 0.5$)

$$\begin{aligned}
\bar{N}_{x,x}^T &= \alpha[(\beta_{121} + \beta_{112})(\bar{T}_0/2) + (\beta_{121} - \beta_{112})(\bar{T}_1/8)] \\
\bar{N}_{y,y}^T &= \beta[(\beta_{221} + \beta_{212})(\bar{T}_0/2) + (\beta_{221} - \beta_{212})(\bar{T}_1/8)] \\
\bar{M}_{x,x}^T &= \alpha[(\beta_{121} - \beta_{112})(\bar{T}_0/8) + (\beta_{121} + \beta_{112})(\bar{T}_1/24)] \\
\bar{M}_{y,y}^T &= \beta[(\beta_{221} - \beta_{212})(\bar{T}_0/8) + (\beta_{221} + \beta_{212})(\bar{T}_1/24)]
\end{aligned} \tag{B-15}$$

Case VII ($z_{nx} > 0.5$, $z_{ny} > 0.5$)

$$\begin{aligned}
\bar{N}_{x,x}^T &= \alpha[(\beta_{111} + \beta_{112})(\bar{T}_0/2) + (\beta_{111} - \beta_{112})(\bar{T}_1/8)] \\
\bar{N}_{y,y}^T &= \beta[(\beta_{211} + \beta_{212})(\bar{T}_0/2) + (\beta_{211} - \beta_{212})(\bar{T}_1/8)] \\
\bar{M}_{x,x}^T &= \alpha[(\beta_{111} - \beta_{112})(\bar{T}_0/8) + (\beta_{111} + \beta_{112})(\bar{T}_1/24)] \\
\bar{M}_{y,y}^T &= \beta[(\beta_{211} - \beta_{212})(\bar{T}_0/8) + (\beta_{211} + \beta_{212})(\bar{T}_1/24)]
\end{aligned} \tag{B-16}$$

Case VIII ($z_{nx} < -0.5$, $z_{ny} < -0.5$)

$$\bar{N}_{x,x}^T = \alpha[(\beta_{121} + \beta_{122})(\bar{T}_0/2) + (\beta_{121} - \beta_{122})(\bar{T}_1/8)]$$

$$\bar{N}_{y,y}^T = \beta[(\beta_{221} + \beta_{222})(\bar{T}_0/2) + (\beta_{221} - \beta_{222})(\bar{T}_1/8)]$$

$$\bar{M}_{x,x}^T = \alpha[(\beta_{121} - \beta_{122})(\bar{T}_0/8) + (\beta_{121} + \beta_{122})(\bar{T}_1/24)]$$

$$\bar{M}_{y,y}^T = \beta[(\beta_{221} - \beta_{222})(\bar{T}_0/8) + (\beta_{221} + \beta_{222})(\bar{T}_1/24)]$$

(B-17)

For a single layer, change β_{112} to β_{111} , β_{122} to β_{121} , β_{212} to β_{211} and β_{222} to β_{221} .

Table 1 Comparison with Boley and Weiner's Results [17] for an Isotropic Single-Layer Thin Rectangular Plate at Different Aspect Ratios ($E_{11}/E_{22} = 1.00$, $\nu_{12} = \nu_{21} = 0.3$, $b/h = 10$)

Aspect Ratio, a/b	Deflection, W/h ($m=n=1$)	
	Boley and Weiner	Present
0.5	0.5300	0.5264
1.0	6.5858	6.5789
1.5	6.3112	6.3063
2.0	2.1104	2.1058

Table 2 Elastic Properties for Two Tire-Cord/Rubber, Unidirectional, Bimodulus Composite Materials^a

Property and Units	Aramid-Rubber		Polyester-Rubber	
	k=1	k=2	k=1	k=2
Longitudinal Young's modulus, GPa	3.58	0.0120	0.617	0.0369
Transverse Young's modulus, GPa	0.00909	0.0120	0.00800	0.0106
Major Poisson's ratio, dimensionless ^b	0.416	0.205	0.475	0.185
Longitudinal-transverse shear modulus, GPa ^c	0.00370	0.00370	0.00262	0.00267
Transverse-thickness shear modulus, GPa	0.00290	0.00499	0.00233	0.00475

^aFiber-direction tension is denoted by $k=1$, and fiber-direction compression by $k=2$.

^bIt is assumed that the minor Poisson's ratio is given by the reciprocal relation.

^cIt is assumed that the longitudinal-thickness shear modulus is equal to this one.

Table 3 Neutral-Surface Positions and Dimensionless Deflections for Rectangular Plates of Single-Layer 0° Aramid-Rubber and Polyester Rubber Determined by Two Different Methods ($b/h=10.0$, $\bar{T}_1=1.0$, $\bar{T}_0=0.0$)

Aspect Ratio a/b	\bar{w}^*		Z_x		Z_y	
	C.F. **	F.E. **	C.F. **	F.E. **	C.F. **	F.E. **
Aramid-Rubber:						
0.5	0.03478	0.03486	0.03059	0.03059	0.2853	0.2807
0.75	0.08147	0.08159	0.04449	0.04441	0.2143	0.2120
1.0	0.1522	0.1523	0.06259	0.06259	0.1332	0.1323
1.25	0.2485	0.2485	0.07970	0.07968	0.07699	0.07699
1.50	0.3624	0.3624	0.08850	0.08849	0.04492	0.04482
1.75	0.4792	0.4790	0.08612	0.08612	0.02843	0.02838
2.0	0.5880	0.5876	0.07491	0.07491	0.01987	0.01986
Polyester-Rubber:						
0.5	0.04815	0.04823	0.1031	0.1030	0.1851	0.1827
0.75	0.1157	0.1158	0.1184	0.1183	0.1068	0.1062
1.0	0.2160	0.2161	0.1308	0.1308	0.05299	0.05276
1.25	0.3410	0.3409	0.1360	0.1360	0.02552	0.02546
1.5	0.4737	0.4736	0.1332	0.1331	0.01285	0.01282
1.75	0.5975	0.5970	0.1234	0.1233	0.007329	0.007329
2.0	0.7024	0.7017	0.1078	0.1078	0.005110	0.005109

* $\bar{w} = Wh/\alpha_1 \bar{T}_1 b^2$

** C.F. denotes closed-form solution; F.E. signifies finite-element solution

Table 4 Neutral-Surface Positions and Dimensionless Deflections for Rectangular Plates of Two-Layer (0°/90°) Aramid-Rubber and Polyester-Rubber Under Sinusoidal Thermal Loading, as Determined by Two Different Methods (b/h = 10.0, $\bar{T}_1 = 1.0$, $\bar{T}_0 = 0.0$)

Aspect Ratio a/b	\bar{w}^*		Z_x		Z_y	
	C.F. **	F.E. **	C.F. **	F.E. **	C.F. **	F.E. **
Aramid-Rubber:						
0.5	--	--	--	--	--	--
0.75	--	--	--	--	--	--
1.0	0.1710	0.1710	0.1198	0.1198	0.03631	0.03468
1.25	0.2602	0.2584	0.1162	0.1162	0.03201	0.03056
1.5	0.3508	0.3492	0.1032	0.1032	0.02873	0.02758
1.75	0.4363	0.4348	0.08413	0.08363	0.02632	0.02523
2.0	0.5139	0.5126	0.06182	0.06161	0.02457	0.02341
Polyester-Rubber:						
0.5	0.09281	0.08935	0.2599	0.2541	0.08784	0.08711
0.75	0.1990	0.1870	0.2554	0.2436	0.08367	0.08356
1.0	0.3090	0.2958	0.2398	0.2294	0.07965	0.07916
1.25	0.3924	0.3816	0.2119	0.2035	0.07645	0.07630
1.5	0.4433	0.4358	0.1734	0.1679	0.07407	0.07311
1.75	0.4719	0.4662	0.1284	0.1252	0.07241	0.07000
2.0	0.4886	0.4833	0.08152	0.08041	0.07136	0.06786

* $\bar{w} = Wh/\alpha_1 t_1 b^2$

** C.F. denotes closed-form solution; F.E. signifies finite-element solution

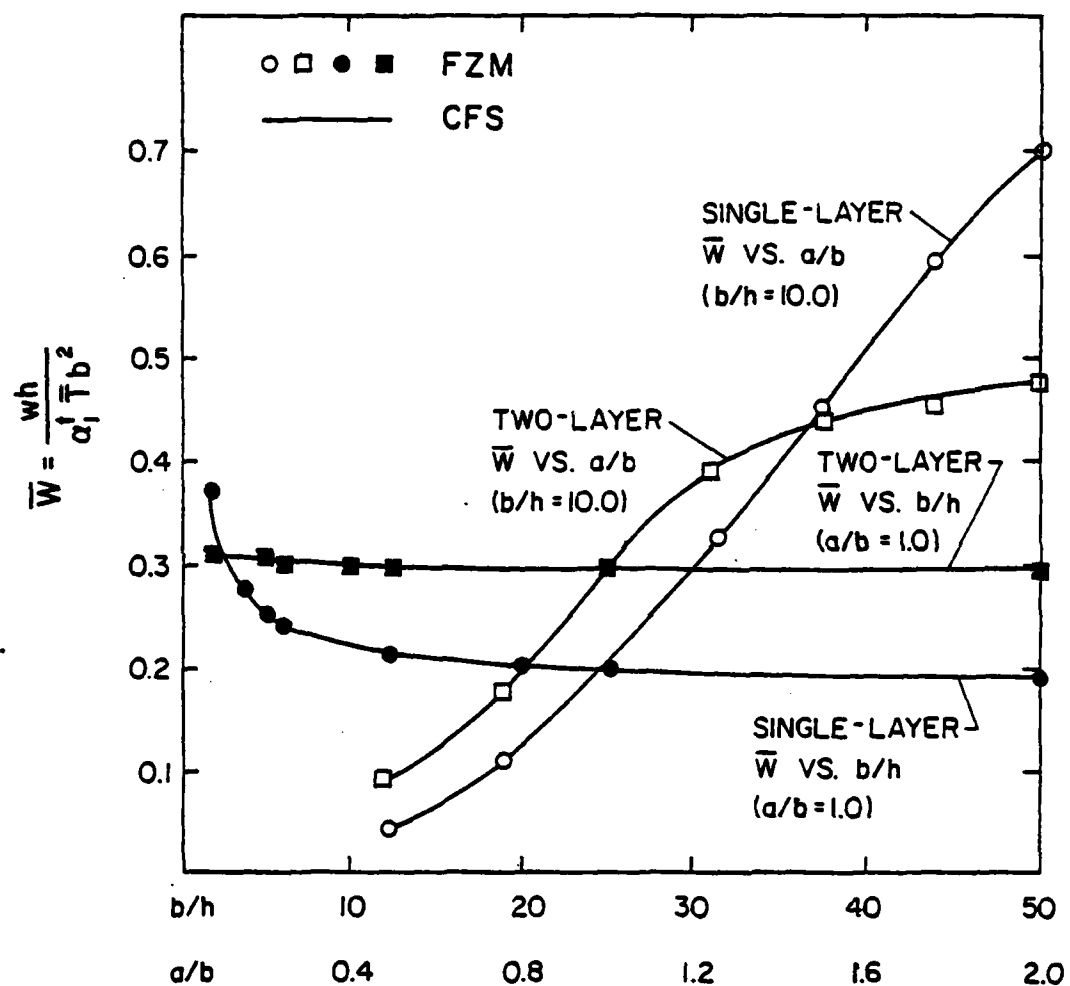


Fig. 1 Transverse deflection vs. aspect ratio (a/b) and side-to-thickness ratio (b/h) for single-layer and two-layer cross-ply plates under sinusoidal thermal loading. (material: polyester-rubber)

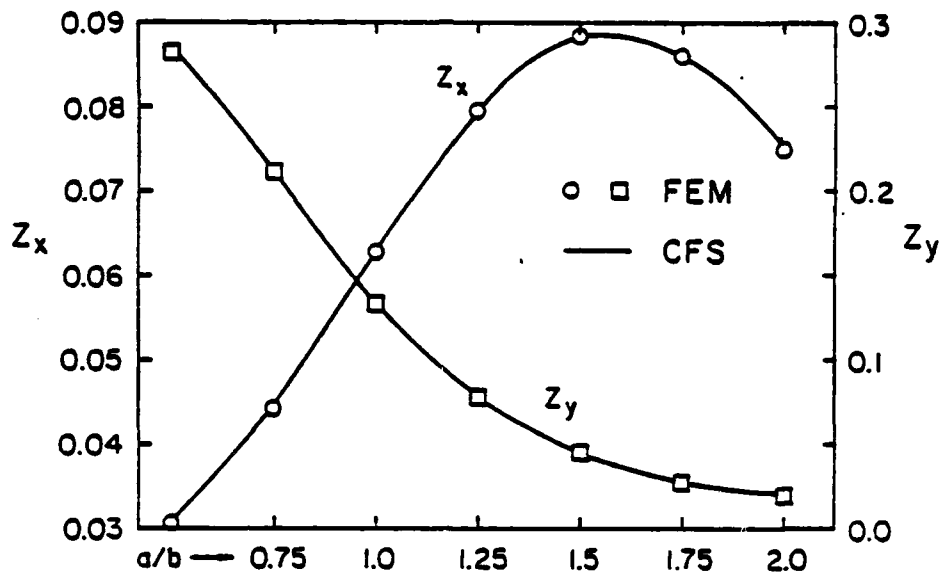


Fig. 2 Neutral-surface location vs. aspect ratio for single-layer (0°) rectangular plates under sinusoidal thermal loading. (material: aramid-rubber, $b/h = 10$)

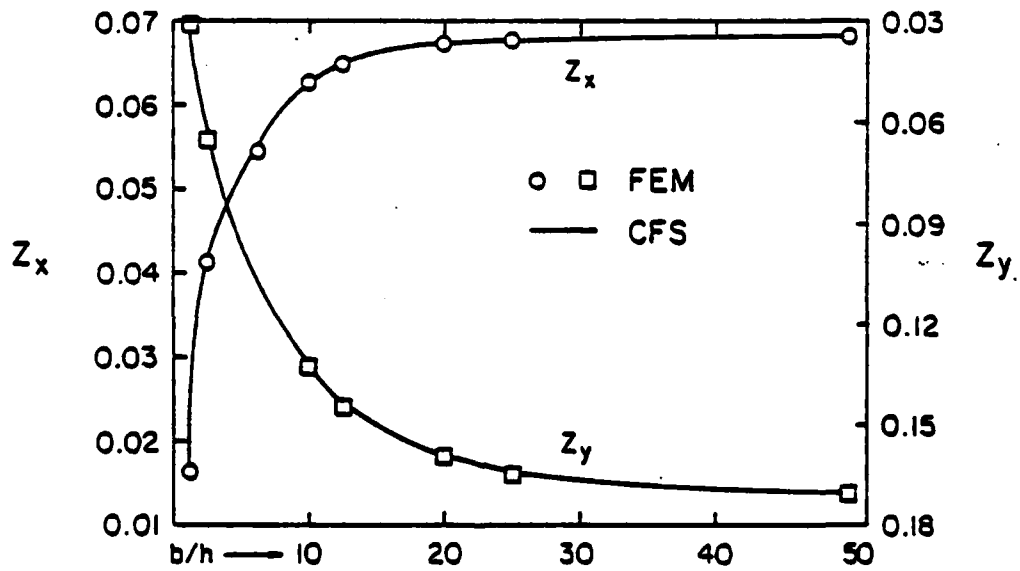


Fig. 3 Neutral-surface location vs. side-to-thickness ratio for single-layer square plates under sinusoidal thermal loading (material: aramid-rubber)

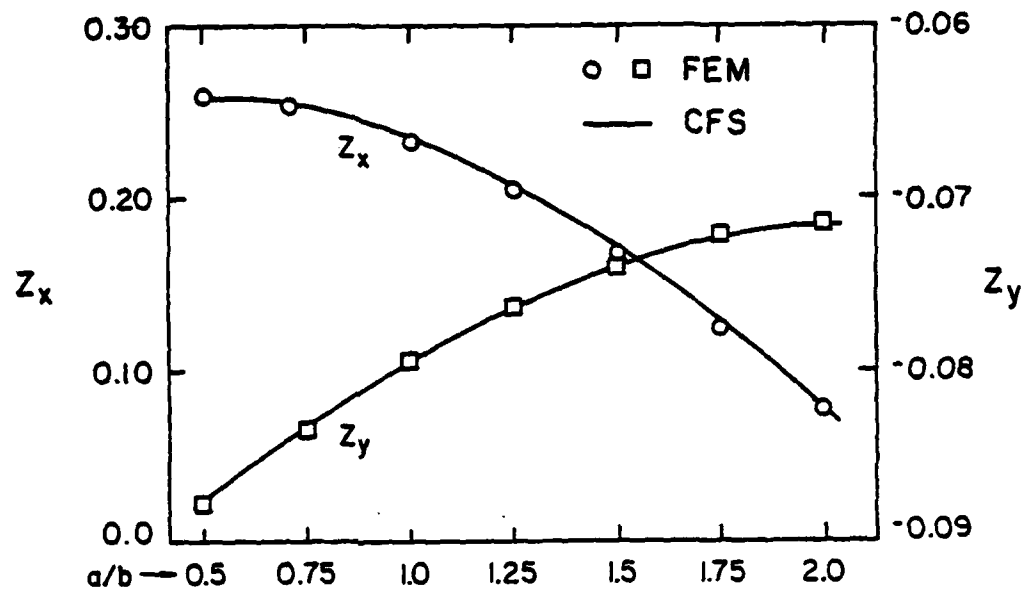


Fig. 4 Neutral-surface location vs. aspect ratio for two-layer cross-ply ($0^\circ/90^\circ$) rectangular plates under sinusoidal thermal loading (material: polyester-rubber, $b/h = 10$)

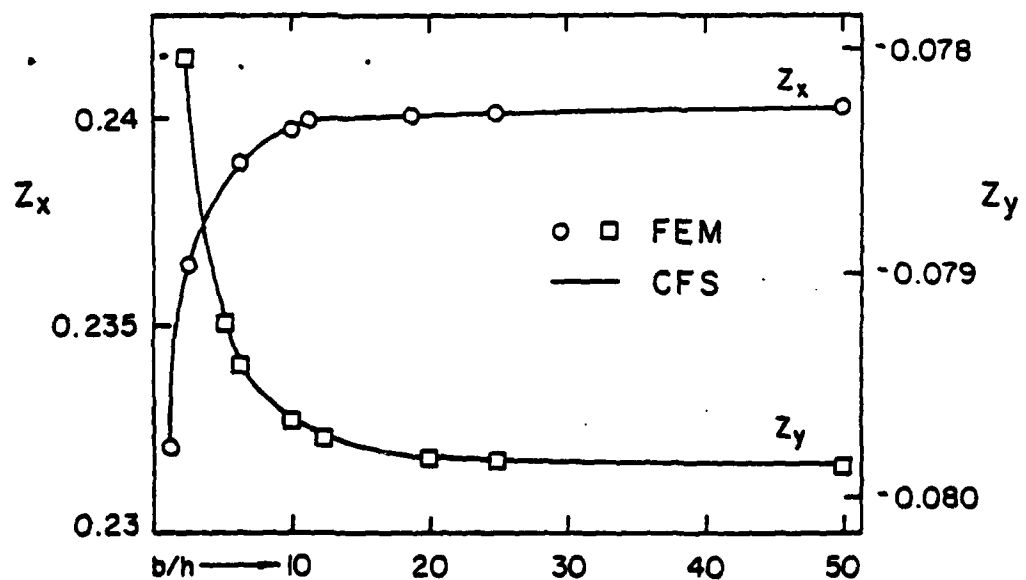


Fig. 5 Neutral-surface location vs. side-to-thickness ratio for two-layer cross-ply ($0^\circ/90^\circ$) square plates under sinusoidal thermal loading (material: polyester-rubber)

PREVIOUS REPORTS ON THIS CONTRACT

Project Rept. No.	OU-AMNE Rept. No.	Title of Report	Author(s)
1	79-7	Mathematical Modeling and Micromechanics of Fiber-Reinforced Bimodulus Composite Material	C.W. Bert
2	79-8	Analyses of Plates Constructed of Fiber-Reinforced Bimodulus Materials	J.N. Reddy and C.W. Bert
3	79-9	Finite-Element Analyses of Laminated Composite-Material Plates	J.N. Reddy
4A	79-10A	Analyses of Laminated Bimodulus Composite-Material Plates	C.W. Bert
5	79-11	Recent Research in Composite and Sandwich Plate Dynamics	C.W. Bert
6	79-14	A Penalty-Plate Bending Element for the Analysis of Laminated Anisotropic Composite Plates	J.N. Reddy
7	79-18	Finite-Element Analysis of Laminated Bimodulus Composite-Material Plates	J.N. Reddy and W.C. Chao
8	79-19	A Comparison of Closed-Form and Finite-Element Solutions of Thick Laminated Anisotropic Rectangular Plates (With a Study of the Effect of Reduced Integration on the Accuracy)	J.N. Reddy
9	79-20	Effects of Shear Deformation and Anisotropy on the Thermal Bending of Layered Composite Plates	J.N. Reddy and Y.S. Hsu
10	80-1	Analyses of Cross-Ply Rectangular Plates of Bimodulus Composite Material	V.S. Reddy and C.W. Bert
11	80-2	Analysis of Thick Rectangular Plates Laminated of Bimodulus Composite Materials	C.W. Bert, J.N. Reddy, V.S. Reddy, and W.C. Chao
12	80-3	Cylindrical Shells of Bimodulus Composite Material	C.W. Bert and V.S. Reddy
13	80-6	Vibration of Composite Structures	C.W. Bert
14	80-7	Large Deflection and Large-Amplitude Free Vibrations of Laminated Composite-Material Plates	J.N. Reddy and W.C. Chao
15	80-8	Vibration of Thick Rectangular Plates of Bimodulus Composite Material	C.W. Bert, J.N. Reddy, W.C. Chao, and V.S. Reddy

UNCLASSIFIED

SECURITY CLASSIFICATION OF THIS PAGE (When Data Entered)

REPORT DOCUMENTATION PAGE		READ INSTRUCTIONS BEFORE COMPLETING FORM	
1. REPORT NUMBER 14 OU-AMNE-89-9, TR-16	2. GOVT ACCESSION NO. AD-A087 425	3. RECIPIENT'S CATALOG NUMBER	
4. TITLE (and Subtitle) 6 THERMAL BENDING OF THICK RECTANGULAR PLATES OF BIMODULUS COMPOSITE MATERIAL	5. TYPE OF REPORT & PERIOD COVERED Technical Report, No. 16		
7. AUTHOR(s) 10 J.N./Reddy & C.W./Bert / Y.S./Hsu and V.S./Reddy	8. CONTRACT OR GRANT NUMBER(s) N00014-78-C-0647		
9. PERFORMING ORGANIZATION NAME AND ADDRESS School of Aerospace, Mechanical and Nuclear Engineering University of Oklahoma, Norman, OK 73019	10. PROGRAM ELEMENT, PROJECT, TASK AREA & WORK UNIT NUMBERS NR 064-609		
11. CONTROLLING OFFICE NAME AND ADDRESS Department of the Navy, Office of Naval Research Structural Mechanics Program (Code 474) Arlington, Virginia 22217	12. REPORT DATE June 1980 12. NUMBER OF PAGES 29 12 32		
14. MONITORING AGENCY NAME & ADDRESS (if different from Controlling Office)	13. SECURITY CLASS. (of this report) UNCLASSIFIED 13a. DECLASSIFICATION/DOWNGRADING SCHEDULE		
16. DISTRIBUTION STATEMENT (of this Report) This document has been approved for public release and sale; distribution unlimited.			
17. DISTRIBUTION STATEMENT (of the abstract entered in Block 20, if different from Report)			
18. SUPPLEMENTARY NOTES			
19. KEY WORDS (Continue on reverse side if necessary and identify by block number) Bimodulus materials, classical solutions, closed-form solutions, composite materials, fiber-reinforced materials, laminated plates, moderately thick plates, rectangular plates, shear flexible plate theory, thermal bending, thermal expansion.			
20. ABSTRACT (Continue on reverse side if necessary and identify by block number) Closed-form and finite-element solutions are presented for thermal bending and stretching of laminated composite plates. The material of each layer is assumed to be elastically and thermoelastically orthotropic and bimodular, i.e., having different properties depending upon whether the fiber-direction normal strain is tensile or compressive. The formulations are based on the thermoelastic version of the Whitney-Pagano laminated plate theory, which includes thickness shear deformations. Numerical results (over)			

DD FORM 1473
1 JAN 79EDITION OF 1 NOV 68 IS OBSOLETE
S/N 0102-014-6001UNCLASSIFIED
SECURITY CLASSIFICATION OF THIS PAGE (When Data Entered)

1100498

JRB

UNCLASSIFIED

SECURITY CLASSIFICATION OF THIS PAGE(When Data Entered)

20. Abstract - Cont'd

are obtained for deflections and neutral-surface positions associated with normal strains in both of the in-plane coordinates. The closed-form and finite-element results are found to be in good agreement.

UNCLASSIFIED

SECURITY CLASSIFICATION OF THIS PAGE(When Data Entered)